

A Perspective Pattern Recognition Using Retinal Nerve Fibers With Hybrid Feature Set

G. Lalli¹, Dr. D.Kalamani², N. Manikandaprabu³

¹Assistant Professor (Sl.G.-II), Dept. of CA, Erode Sengunthar Engineering College, TN, India

²Associate Professor, Dept. of Mathematics, Kongu Engineering College, TN, India

³Lecturer, Dept. of ECE, Senthur Polytechnic College, TN, India

E-mail ID: lalligovindasamy@gmail.com, manikandaprabube@gmail.com

Abstract: This article focuses the implemented concepts for identifying retinal blood vessels based on gray-green channels with Wavelet Transform and Gray-Level Correlation Matrix (GLCM) Texture pattern through Receiver Operating Characteristics (ROC) performance measurement. **Methodological Processes:** The retinal image is preprocessed with resizing. The gray and green channels of a retinal image extracted from either diaretdb0 or diaretdb1 are enhanced by Contrast Limited Adaptive Histogram Equalization (CLAHE). The mathematical morphological operations are performed for acquiring the fine fiber of retinal features with the optic disk, border and noise. The Gray and Green channel based retinal features are further performed by AND logical operations to extract the original noiseless image to count the area cum count of pixels of retinal blood vessels. The 53 functions of Wavelet Transform and 23 functions of Gray-Level Co-occurrence Matrices (GLCM) are individually performed on the area of blood vessels. The best 5 features of each Wavelet Transform functions and GLCM features are considered for further process. 5 best features among these resultant 10 features will be combined with area (count of pixels) of blood vessels are processed by Adaptive Neuro-Fuzzy (ANFIS) training, testing and checking processes. **Result:** Through the performance measures with ROC, the retinal blood vessels will be identified as either 'Authorized' or 'Unauthorized'. **Scope:** Thus this proposed system has an unique systemic processes for retinal vascular structure identification.

[G. Lalli, D.Kalamani, N. Manikandaprabu. **A Perspective Pattern Recognition Using Retinal Nerve Fibers With Hybrid Feature Set.** *Life Sci J* 2013; 10(2):2725-2730]. (ISSN: 1097-8135). <http://www.lifesciencesite.com> 380

Keywords: Wavelet Transform, GLCM, ROC, diaretdb0, diaretdb1, CLAHE, Morphological operations, Adaptive Neuro-Fuzzy

1. Introduction

The biometric system is the most wanted system to get into the venue where the authorized, high-research based progresses are carried out. Such biometric features retinal vascular structure, finger print, iris, palm, signature, gait, etc. are used for determining that the person is authorized or not. These biometric traits have well characteristic properties such as qualitative measurement, distinctiveness, universality, lift-time permanence, etc.

Dr. Carleton Simon and Isodore Goldstein, during their study of eye disease, realized that the person's retinal blood vessels have unique structure from person to person. Subsequently they published an article related to the identification of person in terms of their unique retinal blood vessel patterns (Simon and Goldstein, 1935). Dr. Paul Tower also supports their conclusions in his course of his study of identical twins which done later in the 1950s. He pointed that, of "Any two persons, identical twins would be the most likely to have similar retinal vascular patterns. However, Tower's study showed that of all the factors compared between twins, retinal vascular patterns showed the least similarities (Tower, 1955)^[1-2]".

Retina:

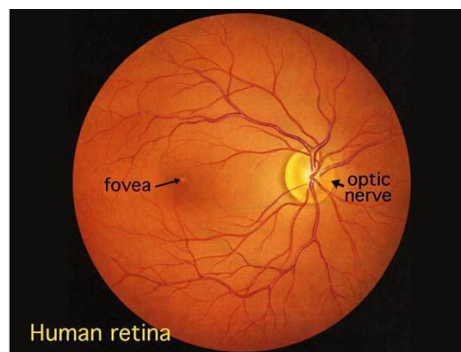


Figure 1. A view of Retina seen through Ophthalmoscope

The optic nerve exists in the center of retina, which is in the shape of circular to oval white area with the measure about 2 x 1.5 mm across. The optic nerve radiates the area of the major blood vessel of retina, which is 17 degrees (4.5-5 mm), or two and half disc diameters to the left of the disc approximately. It can be seen the mere oval-shaped, blood vessel-free reddish spot, the fovea exists at the centre of area of eye termed as macula by ophthalmologists.

Mammalian Retina:

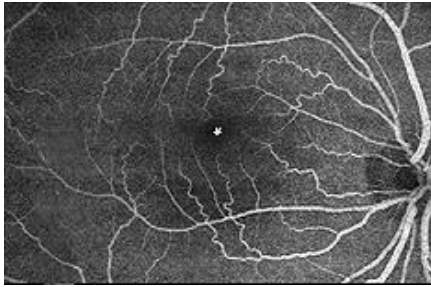


Figure 2. Fundus photograph- flourescein imaging of the major arteries and veins in a normal human right eye retina. (Image courtesy of Isabel Pinilla, Spain)

There are two sources like ‘Central Retinal Artery’ and ‘Choroidal Blood Vessels’ available to supply to the mammalian retina. “The choroid receives the greatest blood flow (65-85%) (Henkind et al., 1979) and is vital for the maintainance of the outer retina (particularly the photoreceptors) and the remaining 20-30% flows to the retina through the central retinal artery from the optic nerve head to nourish the inner retinal layers. The central retinal artery has 4 main branches in the human retina. The vessels in Fig.2. emerge from the Optic nerve head and run in a radial fashion curving towards and around the fovea (asterisk in photograph)^[3]”.

2. The Methodology of Proposed System Retinal Image Processing

This proposed system consists of new sequential methodological processes on retinal digitized image. The following flow illustrates the over all image-oriented process sequences.

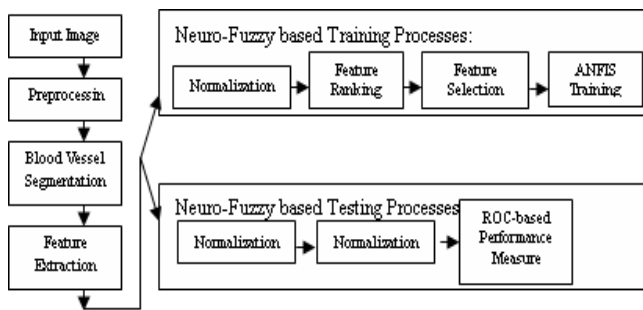


Figure 3. Flow of Image Processing: Training and Testing processes

The fundus retinal images acquired from ophthalmologists or from the databases diaretdb0 and diaretdb1, which have the vast fundus retinal images with above 1200 x 1200. The original size of retina can't be used because of the memory size of the system as well as for further related processes. The

preprocessing is started with resizing of an image with 500 x 500 matrix-based pixels. The segmentation processes consists of Green and Gray or inverted based retinal blood vessels extractions with the enhancement of the blood vessels by using canny-edge detection technique. The features are extracted through the mathematical morphological processes. The normalization process is followed for fixing the feature value in between 0 and 1, which is the unit interval. The area or count of blood vessels is calculated. Two different kinds of techniques such as wavelet transformation and gray-level co-occurrence matrices are used for feature ranking on retinal blood vessels. The feature selection process is carried out with the technique of linear discriminant analysis. The adaptive neuro-fuzzy inference system is used for training the features. Similarly the neuro-fuzzy based testing is used for identifying the authorization, the decision made at certain epoch level convergence of this biometric system.

3. Methodologies Used

3.1. Databases (diaretdb0 and diaretdb1)

The Standard Diabetic Retinopathy Database (Calibration Level 0) named ‘diaretdb0’ and Standard Diabetic Retinopathy Database (Calibration Level 1) named ‘diaretdb1’ have retinal fundus images. The diaretdb0 has 130 color images. All fundus images were acquired using a Zeiss FF450+ fundus camera^[4]. The diaretdb1 has 89 color images. The pixels at 24 bit RGB, captured using a 50° field-of-view digital fundus camera^[5]. In this article both the original images and these database related images are used for training and testing the images for authentication of a person in terms of retinal blood vessels.

3.2. Image: Green and Gray Channels Extraction

The resized fundus image is converted in two different ways as separate processes. One is rgb-to-gray for gray channel extraction and another is RGB for green channel extraction.

3.3. Contrast Limited Adaptive Histogram Equalization (CLAHE)

In both way of separate serial processes, the contrast-limited adaptive histogram equalization (CLAHE) is used for enhancing the extracted image. “ $J = \text{adapthisteq}(I)$ enhances the contrast of the grayscale image I by transforming the values using CLAHE. CLAHE operates on small regions in the image, called *tiles*, rather than the entire image. Each tile's contrast is enhanced, so that the histogram of the output region approximately matches the histogram specified by the 'Distribution' parameter. The neighboring tiles are then combined using bilinear interpolation to eliminate artificially induced boundaries. The contrast, especially in homogeneous areas, can be limited to avoid

amplifying any noise that might be present in the image^[6]».

3.4. Mathematical Morphological Processes

The unwanted parts such as optical disk and border of retinal image are removed with the help of mathematical morphological operations. The specific MATLAB-based operations like ‘ball’ and ‘disk’ are used with the values r=6 and radius value=6 for disk and border removal respectively.

3.5. Median Filter for Noise Removal

Median filtering is widely used in digital image processing with the restriction while acquire and preserves edges for removing noise^[7-8].

Formula: $MEDIAN = \{ (n + 1) / 2 \}$ th item;
n = number of values.

Fig. Noise Removal in Pixel-based Matrices with Red and Green Channels (Row-wise Process)

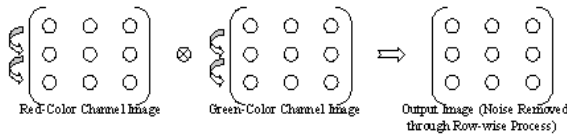


Fig. Noise Removal in Pixel-based Matrices with Red and Green Channels (Column-wise Process)

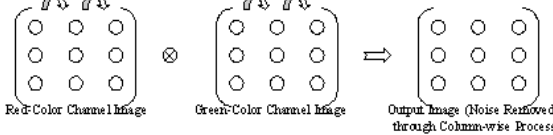


Figure 4. Noise Removal Processes

3.6. Canny Edge Detection

The first step is to filter out any noise in the original image before trying to locate and detect any edges. The Sobel operator uses a pair of 3x3 convolution masks, one estimating the gradient in the x-direction (columns) and the other estimating the gradient in the y-direction (rows). They are shown below:

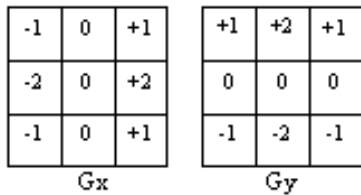


Figure 5. Edge Detection Matrices

The magnitude, or EDGE STRENGTH, of the gradient is then approximated using the formula:

$$|G| = |G_x| + |G_y|$$

The formula for finding the edge direction is just:

$$\theta = \text{invtan} (G_y / G_x)$$

3.7. Blood Vessel Area Calculation

The matrix of image is labeled as a[100x100]. The below procedure can be used to calculate the area of blood vessels ie. the existence of the number of pixels.

$$x=1:100 \quad \& \quad y=1:100$$

if (a[x,y] ==1) then area=area+1.

3.8. Logical AND Operation

The ‘AND’ operation is performed on the features of the extracted images through two different ways of below represented System flow processes.

Table 1. Truth Table (AND Logic Operation)

Truth Table: AND Logic		
Inputs		Output
In ₁	In ₂	Out
0 (False)	0 (False)	0 (False)
0 (False)	1 (True)	0 (False)
1 (True)	0 (False)	0 (False)
1 (True)	1 (True)	1 (True)

The ‘AND’ operation is performed on the features of the extracted images through two different ways of System flow processes using gray/green channel extraction or using complement.

3.9. Wavelet Transformation

The wavelet transform is similar to the Fourier transform (or much more to the windowed Fourier transform) with a completely different merit function. The main difference is this: Fourier transform decomposes the signal into sines and cosines, i.e. the functions localized in Fourier space; in contrary the wavelet transform uses functions that are localized in both the real and Fourier space. Generally, the wavelet transform can be expressed by the following equation:

$$F(a, b) = \int_{-\infty}^{\infty} f(x) \psi_{(a,b)}^*(x) dx$$

where the * is the complex conjugate symbol and function ψ is some function. This function can be chosen arbitrarily provided that obeys certain rules^[9].

The retinal fundus image features are extracted by using the efficient wavelet transform functions such as rbio1.1, rbio1.3, bior3.7, bior1.3 and coif1. Features of an image can be efficiently processes through Wavelet^[18-19].

3.10. GLCM

Gray Level Co-Occurrence Matrix (GLCM) used for image classification can also be referred as a co-occurrence distribution. It is defined over an image for the distribution of co-occurring values at a user-specific offset other hand it represents the distance as well as angular spatial relationship over an image sub-region of specific size. The GLCM is organized from a

gray-scale image. The GLCM is calculates how over and over again a pixel with gray-level (grayscale intensity or Tone) value i occurs either horizontally, vertically, or diagonally to adjacent pixels with the value j ^[10]. Textural Features are quite helpful for image classification^[20].

Directions of Analysis with GLCM

1. Horizontal (00)
 2. Vertical (900)
 3. Diagonal:
 - a) Bottom left to top right (-450)
 - b) Top left to bottom right (-1350)
- Denoted P0, P45, P90, & P135 Respectively.
Ex. P90(i, j)^[11-12].

The efficient properties named autocorrelation, sum entropy, inverse-difference normalized, inverse-difference moment normalized and homogeneity of GLCM are used for classifying and extracting the gray level images and its' features respectively.

3.11. ANFIS

Adaptive neuro fuzzy inference system (ANFIS) is a type of neural network based on Takagi–Sugeno fuzzy inference system. It integrates both neural networks and fuzzy logic principles. Hence, it has potential to capture the benefits of both the neural network and fuzzy logic in a single framework. Its inference system corresponds to a set of fuzzy IF–THEN rules that have learning capability to approximate nonlinear functions^[13]. Hence, ANFIS is considered to be a universal estimator^[14].

3.11.1. Subtractive clustering

Subtractive clustering is one among the automated data-driven based methods for organizing the core fuzzy models proposed by chiu^[15]. It is an extension of the Mountain Clustering technique, which is intraduced by Yager and Filev^[16]. This method avoids from rule-base explosion problem. It is a fast, one-pass algorithm for estimating the number of clusters and the cluster centers in a set of data.

The main processes of subtractive clustering are as follows:

The algorithm assumes each data point is a potential cluster center and calculates some measure of potential for each of them according to the following equation.

$$P_i = \sum_{j=1}^m \exp^{-\alpha \|x_i - x_j\|}$$

Where, $\alpha = 4 / r_a^2$ and $r_a > 0$ defines the neighborhood radius for each cluster center, while it has a set of m data points $\{x_1, \dots, x_m\}$ in a N -dimensional space^[17].

4. Systemic Resultant Values

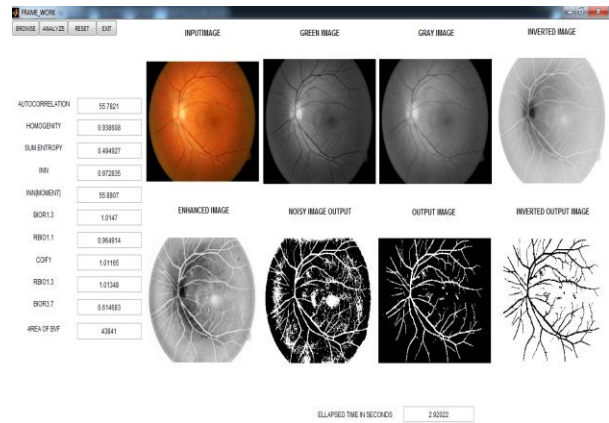


Figure 6. Systemic Implementation of retinal image

Table 2. GLCM (Features)

Particulars	GLCM Functions (Ordered-Best 5 performances)				
	Autocorrelation	Sum Entropy	Inverse-Difference Normalized (INN)	Inverse-Difference Moment Normalized	Homogeneity
Img1	60.8187331	0.245804	0.988244	60.90945	15.44065
Img2	60.6805386	0.251245	0.989997	60.71946	15.38794
Img3	61.4062161	0.209598	0.990351	61.50695	15.54475
Img4	61.8802676	0.17738	0.993148	61.91077	15.61497
Img5	58.0242717	0.285107	0.985915	60.27372	15.31928
Img6	55.7821138	0.256669	0.988733	60.71305	15.38899
Img7	58.943208	0.227306	0.990118	61.09464	15.48167
Img8	60.1409383	0.287748	0.986297	60.07448	15.3019
Img9	58.2041497	0.28324	0.987201	60.20696	15.30535
Img10	58.4073171	0.204098	0.992974	61.44648	15.51826

Table 3. Wavelet Transform (Features)

Particulars	Wavelet Transform Functions (Ordered-Best 5 performances)				
	rbio1.1	rbio1.3	bior3.7	bior1.3	coif1
Img1	1.77E-05	1.79E-05	3.35E-05	1.87E-05	1.82E-05
Img2	2.82E-05	2.74E-05	3.97E-05	2.8E-05	2.76E-05
Img3	7.02E-06	6.74E-06	1.88E-05	7.23E-06	6.89E-06
Img4	6E-07	4.32E-07	1.32E-06	4.34E-07	3.88E-07
Img5	9.32E-06	8.74E-06	2.37E-05	9.71E-06	9.06E-06
Img6	1.57E-06	1.44E-06	5.2E-06	1.63E-06	1.52E-06
Img7	6.19E-07	6.05E-07	1.64E-06	6.56E-07	6.35E-07
Img8	2.13E-06	1.97E-06	5.87E-06	2.21E-06	2.19E-06
Img9	5.88E-06	5.96E-06	1.5E-05	6.54E-06	6.04E-06
Img10	1.32E-06	1.42E-06	3.21E-06	1.51E-06	1.47E-06

Table 4 Hybrid Results (Wavelet Transform – GLCM)

Particulars	Hybrid (WT-GLCM)					
	Autocorrelation	Homogeneity	Sum Entropy	bior1.3	rbio1.1	Area of Blood Vessels Count of Pixels
Img1	60.8187331	15.44065	0.245804	1.87E-05	1.77E-05	19643
Img2	60.6805386	15.38794	0.251245	2.8E-05	2.82E-05	8257
Img3	61.4062161	15.54475	0.209598	7.23E-06	7.02E-06	17349
Img4	61.8802676	15.61497	0.17738	4.34E-07	6E-07	24774
Img5	58.0242717	15.31928	0.285107	9.71E-06	9.32E-06	32115
Img6	55.7821138	15.38899	0.256669	1.63E-06	1.57E-06	21945
Img7	58.943208	15.48167	0.227306	6.56E-07	6.19E-07	16867
Img8	60.1409383	15.3019	0.287748	2.21E-06	2.13E-06	10756
Img9	58.2041497	15.30535	0.28324	6.54E-06	5.88E-06	14402
Img10	58.4073171	15.51826	0.204098	1.51E-06	1.32E-06	25754

The above tables have values for 10 images which are implemented through wavelet transformation and GLCM techniques. But the implementation is done for 219 images by using these two techniques for extracting the best features.

5. Future-System Performance Evaluation

The patterns may be matched in terms of “Sensitivity” and “Specificity” to determine the accuracy as well as for authentication and authorization.

Input Image	Desired Value		Decision		Percentage	
	Positive	Negative				
Actual Value	Positive (True)	P	P ¹	Authorization	$P / (P + P^1)$	0.99 (99%)
	Negative (False)	N ¹	N	Unauthorization	$N / (N^1 + N)$	1 (100%)
ROC		Sensitivity	Specificity	Accuracy = $(P + N) / (P + P^1 + N^1 + N)$		
Percentage		1 (100%)	0.99 (99%)			0.99 (99%)

Figure 7. Performance Measure with ROC

Sensitivity: Test-Matching Process is Positive. The Patterns are matched.

Specificity: Test-Matching Process is Negative. The Patterns are mismatched.

These concepts may be determined according to the following formulae:

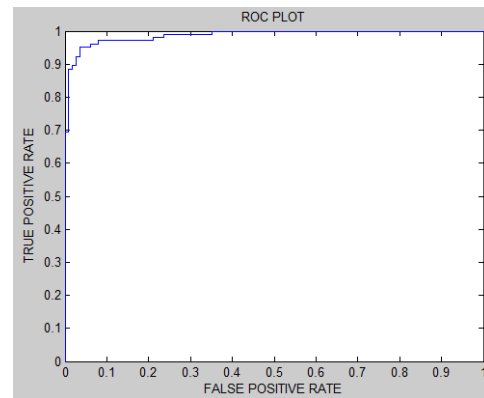
$$\begin{aligned} \text{Sensitivity (Se)} &= P / (P + N^1) \\ &= 100\% \\ \text{Specificity (Sp)} &= N / (P^1 + N) \\ &= 99\% \end{aligned}$$

$$\begin{aligned} \text{Authorization} &= P / (P + P^1) \\ &= 99\% \end{aligned}$$

$$\begin{aligned} \text{Unauthorization} &= N / (N^1 + N) \\ &= 100\% \end{aligned}$$

$$\begin{aligned} \text{Accuracy} &= (P + N) / (P + P^1 + N^1 + N) \\ &= 99\% \end{aligned}$$

The ROC is plotted for classification representation with the consideration of best two functional features such as sum entropy of wavelet transformation and inverse difference normalized of GLCM as follows. The Receiver Operating Characteristics (ROC) Plot and the Area Under the ROC Curve (AUC) is also calculated and mentioned in the figure of ROC plot.



AUC = 0.9875

Figure 8. ROC Plot for Classification

6. Conclusion

The retinal blood vascular structure of a person can be determined by detecting the pattern matching process in between the stored and the current generated images. For the accurate identification of an image, the gray and green channel features are implemented and compared through the count of blood vessels in the processed area. The Neuro-Fuzzy and ROC performance related processes on Wavelet Transformation and GLCM based features are also considered for accurate measurement for retinal blood vessels in terms of its' featured identification.

Corresponding Author:

G. Lalli, M.C.A., M.Phil., (Ph.D.),
Assistant Professor (Selection Grade-II),
Erode Sengunthar Engineering College,
Thudupathi (Post), Erode (District) PIN: 638 057.
Tamil Nadu (State), India.

References:

[1] De Schaeplrijver, L., Simoons, L. P., Lauwers, H.,

- and DeGesst, J. P. 1989. Retinal vascular patterns in domestic animals. *Res. Vet. Sci.*, 47:34-42.
- [2] Family, F., Masters, B. R., Platt, D. E. 1989. Fractal pattern formation in human retinal vessels. *Physica D* 38:98-103.
- [3] Helga Kolb, "Simple Anatomy of Retina".
- [4] Kauppi, T., Kalesnykiene, V., Kamarainen, J.-K., Lensu, L., Sorri, I., Uusitalo, H., Kälviäinen, H., Pietilä J., *DIARETDB0: Evaluation Database and Methodology for Diabetic Retinopathy Algorithms*, Technical report
- [5] Kauppi, T., Kalesnykiene, V., Kamarainen, J.-K., Lensu, L., Sorri, I., Raninen A., Voutilainen R., Uusitalo, H., Kälviäinen, H., Pietilä J., *DIARETDB1 diabetic retinopathy database and evaluation protocol*, Technical report.
- [6] Zuiderveld, Karel. "Contrast Limited Adaptive Histogram Equalization." *Graphic Gems IV*. San Diego: Academic Press Professional, 1994. 474–485.
- [7] E. Arias-Castro and D.L. Donoho, "Does median filtering truly preserve edges better than linear filtering?", *Annals of Statistics*, vol. 37, no. 3, pp. 1172–2009.
- [8] G.R. Arce, "Nonlinear Signal Processing: A Statistical Approach", Wiley:New Jersey, USA, 2005.
- [9] A. Bultheel: *Bull. Belg. Math. Soc.*: (1995), p2.
- [10] <http://www.mathworks.com/access/helpdesk/help/toolbox/images/index.html?/access/helpdesk/help/toolbox/images/graycomatrix.html&http://www.google.com/search?hl=en&client=firefox-a&rls=org.mozilla:en-US:official&hs=O&sa=X&oi=spell&resnum=0&ct=result&cd=1&q=grayscale+cooccurrence+matrix+example&spell=1>
- [11] <http://www.fp.ucalgary.ca/mhallbey/tutorial.htm>
- [12] <http://www.fp.ucalgary.ca/mhallbey/examples.htm>
- [13] Nedjah, Nadia (ed.). *Studies in Fuzziness and Soft Computing*. Germany: Springer Verlag. pp. 53–83. ISBN 3-540-25322-X. Text "Adaptation of Fuzzy Inference System Using Neural Learning, Fuzzy System Engineering: Theory and Practice " ignored (help)
- [14] Jang, Sun, Mizutani (1997) – *Neuro-Fuzzy and Soft Computing* – Prentice Hall, pp 335–368, ISBN 0-13-261066-3
- [15] Chiu, S., 1994. "Fuzzy Model Identification Based on Cluster Estimation," *Journal of Intelligent & Fuzzy Systems*, Vol. 2, No. 3, Spet.
- [16] Yager, R. Filev, D., 1994. Generation of fuzzy rules by mountain clustering, *J. Intell. Fuzzy Syst.* 2 (3), 209–219.
- [17] Hossein Abbasimehr, Mostafa Setak and M. J. Tarokh "A Neuro-Fuzzy Classifier for Customer Churn Prediction" *International Journal of Computer Applications*, (0975-8887) Vol: 19 No. 8, April 2011 Pages: 35-41.
- [18] Mostafa Sadeghi1 and Faezeh Memarzadehzavareh "Applying Wavelet in Image Processing For Visible Defect Detection on Steel Surfaces" *Life Sci J* 2013;10(2s):356-359. (ISSN: 1097-8135).
- [19] Bharat Bhosale, Bouthina Ahmed and Anjan Biswas "On Wavelet based modeling of Neural networks using Graph theoretic approach" *Life Sci. J.* 2013; 10(2):1509-1515]. (ISSN: 1097-8135).
- [20] Robert M. Haralick, K. Shanmugam and Its'hak Dinstein "Textural Features for Image Classification", *IEEE Transactions on Systems, Man and Cybernetics* Vol. SMC-3, No. 6, November 1973, pp.610-621.

6/20/2013